Statistical beam information for mmW positioning

Ramón A. Delgado*, Torbjörn Wigren†, Katrina Lau*, Richard H. Middleton*, Iana Siomina†
*School of Electrical Engineering and Computing, *The University of Newcastle*. Australia
Email: {ramon.delgado, k.lau, richard.middleton}@newcastle.edu.au
† *Ericsson AB*, Stockholm, SE-16480, Sweden.
Email: {torbjorn.wigren, iana.siomina}@ericsson.com

***Abstract*—This paper proposes to collect statistical information of beam usage from multiple base stations for user localization at mmW carrier frequencies. This information is then used to construct multidimensional histograms that capture the correlations between good beam directions from multiple base stations. The histograms can be used to reduce the complexity of the multiple beam searches required for mmW positioning. Simulation results suggest that the multidimensional histograms are sparse, with only a few dominating beam directions. In light of this insight, methods are proposed to reduce the time needed to locate a mobile terminal when the observed time difference of arrival method is used for positioning.**

***Index Terms*—Beamforming, positioning, localization, mmW, OTDOA.**

I. Introduction

The 5G new radio (NR) telecommunication system will operate at millimeter Wave (mmW) carrier frequencies where there is plenty of available spectrum to meet the requirements of traditional mobile broadband applications with enhanced performance [1]. In addition, applications requiring ultra reliable low latency communications [2], [3] are supported due to very low symbol times. One of the main technologies associated with mmW carrier frequencies is the use of large antenna arrays that provide high directivity and a significant beamforming gain helping to compensate for the shrinking antenna element areas and shadowing occurring at mmW frequencies [1], [4]. Under these circumstances, the beams at a transmitter and a receiver node need to align with each other to establish communication. The search for the combination of beam directions in the user equipment (UE) and the base station that results in the best signal-to-noise ratio requires evaluation of a possibly large space of beam combinations.

With the arrival of 5G, it is expected that the Assisted Global Navigation Satellite System (AGNSS) will be increasingly augmented with localization techniques based on mobile telecommunication network measurements [5]. This will help to improve positioning accuracy indoors and in dense urban environments. The high bandwidth radios that are anticipated for NR, together with the large antenna arrays applied at mmW frequencies, will result in high accuracy ranging information, together with high accuracy directional information. This will allow single site, short range, high accuracy localization indoors and outdoors that can meet also new vertical emergency (E-911) requirements [5]. For longer range rural outdoor E-911 and lawful intercept localization, time difference of arrival (TDOA) methods also relying on high radio bandwidths are believed to be needed. However, here coverage and range will be very challenging also for mid-frequency bands [6], requiring narrow antenna lobes with very high gain. The same challenge exists in more urban environments when mmW carrier frequencies are used. Both cases increase the space of the beam search significantly, which is a main motivation for the present paper.

To explain this in more detail, note that high accuracy TDOA positioning algorithms applied in mobile communication networks rely on multilateration. This means that a UE seeking to estimate its position needs to get measurements from at least three base stations to obtain a horizontal position, while theoretically four base stations are needed to obtain a three-dimensional (3D) position [5]. In practice, more than four base stations are often needed before a position fix is computed [5]. In case 3D localization with E-911 accuracy is needed in rural areas, additional fusion with altitude maps is typically needed as well [6]. At mmW carrier frequencies beamforming with maximum gain is believed to be needed to detect signals from base stations far away, potentially requiring a very significant amount of time for beam search and time of arrival acquisition. This may make it difficult to comply with positioning specifications such as E-911 that require accurate positioning in less than 30 seconds [5]. For an overview of methods and challenges for positioning in NR networks, the reader is referred to [5]–[8].

As mentioned above, a likely approach to offer location-based services in NR is to use observed TDOA (OTDOA) positioning. A UE estimates the distance to each base station by measuring the time differences between the measured time of arrivals of positioning reference signals from each pair of base stations [5]. Since time information needs to be measured in the UE w.r.t. several base stations, a beam search is required for each base station in the UE. Note that in case the UE applies receiver beamforming, the search space is the product of the UE and base station beam spaces. Note again that non-serving cell transmitters are likely to need to use narrow beams to allow detection over long distances.

This paper proposes collection of statistical data of the beam directions of the base stations used during *successful* positioning attempts. This data is then used to construct histograms of the beam directions probabilities, i.e. indicating in which beam direction a UE is likely to be found. These histograms can assist beam search by reducing the search space. Additionally, a multi-site statistical information measure on

Peer-reviewed author's copy of:
R. A. Delgado, T. Wigren, K. Lau , R. H. Middleton and I. Siomina. **Statistical beam information for mmW positioning**. In *IEEE 91st Vehicular Technology Conference (VTC2020-Spring)*, 2020.
Available at https://doi.org/10.1109/VTC2020-Spring48590.2020.9129626
©2020 IEEE. Personal use of this material is permitted. Permission from IEEE must be obtained for all other uses, in any current or future media, including reprinting/republishing this material for advertising or promotional purposes, creating new collective works, for resale or redistribution to servers or lists, or reuse of any copyrighted component of this work in other works.

the successful beam directions is suggested. This information is used to compute the beam directions at which a UE is most likely to be found given that the UE is connected to a site at a specific beam direction. The method exploits the high correlation existing between multi-site beam directions caused by the geometry of the environment, in particular in indoor and urban environments where many reflected mmW beams are expected to exist. This allows a UE to obtain measurements for positioning from several base stations in a reduced amount of time.

II. OTDOA for mmW positioning

OTDOA is a downlink positioning method that relies on time difference of arrival measurements obtained from pilot signals transmitted from multiple base stations positioned at known locations. Since the NR standardization is not yet completed, the 4G LTE system is used for the description of the present paper.

In LTE OTDOA the UE measures the reference signal time difference (RSTD) between two base stations. Each base station transmits Position Reference Signals (PRS) which are measured in downlink by the UE. To obtain RSTD measurements, the base stations in the network need to be synchronized with each other, or the time of transmission differences denoted the real time differences (RTD) need to be measured by location measurement units (LMUs) at known locations [5]. To estimate two UE coordinates at least three RSTD measurements are needed from base stations at different locations. The measurements are used to intersect hyperbolas generated with the RSTD measurements, and the solution is unique unless the base stations locations are in degenerate subspaces. In practice, RSTD measurements may contain errors due to imperfect network synchronization, non-line-of-sight measurements, and additive measurement noise. Thus, redundant RSTD measurements are usually needed for accurate position estimation [5]. A further challenge occurs when OTDOA is used for 3D localization. Since the participating base stations are then often located at comparable altitudes, the same is true for their antenna positions. As is well known, this leads to a poor vertical geometry (poor vertical dilution of precision, GDOP [9]). A solution to this problem is to fuse vertical map information with the OTDOA positioning equations, e.g. as in [6].

As motivated in the introduction, a reduction of the time required to detect PRS will significantly reduce the time needed to collect enough RSTD measurements. In passing, it is noted that a search space reduction also increases the detection sensitivity, by a reduction of the false alarm rate, c.f. [5]. In the following sections the focus is therefore on methods to reduce the time required to perform OTDOA measurement.

III. Collecting Beam Direction Statistics

This section describes the method to collect statistical information of the base station beam directions used during successful positioning attempts. The information collected is then used to reduce the number of beam directions on which the PRSs are transmitted.

A. Single site statistical information

This section describes how to compute a histogram for a single base station. Consider a non-overlapping partition of the space of beam directions $\{\Omega_i\}_{i=1}^n$ with each set in the partition containing one or more beam directions. Next consider that M reports of PRS measurements are provided by the UEs, and each report has a base station beam direction α_k with $k = 1, \ldots, M$. Thus, a histogram based on $\{\Omega_i\}_{i=1}^n$ can be constructed as a vector $\mathbf{h} \in \mathbb{R}^n$ with elements $\mathbf{h}(i)$ that count the number of beam directions α_k such that $\alpha_k \in \Omega_i$, i.e.

$$\mathbf{h}(i) = \sum_{k=1}^{M} \mathbb{I}(\alpha_k \in \Omega_i) \tag{1}$$

where $\mathbb{I}(condition)$ is an indicator function taking the value 1 if the *condition* is true and taking the value zero otherwise. Although (1) constructs a histogram by accumulating a batch of measurements, the histogram can be updated one sample at a time making the method suitable for online implementation.

At mmW, radio propagation shows a beam-like behavior, with effects of reflection and diffraction that resemble those of light. This implies that the histogram $\mathbf{h}$ is influenced by the geometry of the environment and by aggregated moving patterns of the UEs requesting positioning.

B. Multi-site statistical information

The high correlation between the geometry of the environment and the radio propagation characteristics may be used to relate beam directions of neighboring base stations. To do so, it is proposed to keep track of the statistics of beam directions of PRSs measured by a UE, for neighbor base stations. In a similar fashion to that for a single base station, it is proposed to use multidimensional histograms to keep track of the statistics of two neighbor base stations. Consider a non-overlapping partition of the space of feasible beam directions $\{\Omega_i^A\}$ for $i = 1, \ldots, n_a$ for a base station A and $\{\Omega_j^B\}$ for $i = 1, \ldots, n_b$ for a base station B. Next, a UE reports to the network the beam direction α on which the user successfully received PRS measurement for base station A and the beam direction β on which the PRS measurement for base station B was obtained. Then, M reports of RSTD measurements are provided by the UEs, and each such report has a pair of beam directions (α_k, β_k) with $k = 1, \ldots, M$. Based on these reports, a two-dimensional histogram can be generated as a matrix $\mathbf{H} \in \mathbb{R}^{n_a \times n_b}$ on which each matrix element is given by

$$\mathbf{H}(i,j) = \sum_{k=1}^{M} \mathbb{I}\left(\alpha_k \in \Omega_i^A \; and \; \beta_k \in \Omega_j^B\right) \tag{2}$$

Histograms may be constructed between each pair of neighbor base stations. Alternatively, higher-dimensional tensor data structures may be used to keep statistics relating more than two base stations. These histograms and tensors capture the relationships between beam directions of neighbor base stations.

IV. Managing beam search

A. Single-site beam search management

Statistical information from a single site can now be used to guide the beam search. Beam directions that more often lead to successful PRS measurements can be given priority over less successful beam directions. Prioritized beam directions may be explored before any non-prioritized beam directions. In most cases the beam search will succeed using only prioritized beam directions, resulting in a reduced number of attempts compared to the case when no prioritization is used. When no feedback is provided by the UE about successful beam measurements or that the beam space is explored using a random search, prioritized beam directions can be explored more often than non-prioritized directions.

B. Multi-site beam search management

Multi-site statistical information may also be used to guide the beam search across multiple sites. The multi-site statistical data described earlier captures the relationship between the beam directions in one site and the beam directions in another site. Therefore, knowledge about successfully measured PRSs from one site may reduce the number of attempted beam directions until a PRS is measured in a second site. The details are described in Algorithm 1.

Algorithm 1: Multi-site beam search.

Data: A priority threshold $T_{priority}$ and multi-site Histogram $\mathbf{H}$.

```
/* Priority scan                                   */
for i = 1,...,n_a do
    for j = 1,...,n_b do
        for k = 1,...,n_c do
            if H(i,j,k) > T_priority then
                Send order to sites to transmit in the
                  directions corresponding to H(i,j,k);
                Transmit PRS from each site;
                Attempt to compute OTDOA position;
                if Successful position computation then
                    stop and exit;
/* Uniform low priority scan                       */
for i = 1,...,n_a do
    for j = 1,...,n_b do
        for k = 1,...,n_c do
            if H(i,j,k) ≤ T_priority then
                Send order to sites to transmit in the
                  directions corresponding to H(i,j,k);
                Transmit PRS from each site;
                Attempt to compute OTDOA position;
                if Successful position computation then
                    stop and exit;
```

C. Expected number of steps

Consider that there are N beam direction combinations where a UE can be found with probability $\mathbf{P}_k$ for $k = 1, \ldots, N$ and that the beam directions are explored according to the sequence $\{s_k\}_{k=1}^N$. A benchmark case can be considered when $\mathbf{P}_k = 1/N$ for all k, in which case for any sequence $\{s_k\}_{k=1}^N$ the average number of steps to find a UE is $\tau_b = (N+1)/2$. To compute the expected number of steps for Algorithm 1, $\tau_1 = \sum_{k=1}^N k\mathbf{P}_{s_k}$, it is useful to express it as

$$\tau_1 = \sum_{k=1}^{L} k\mathbf{P}_{s_k} + \sum_{k=L+1}^{N} k\mathbf{P}_{s_k}, \tag{3}$$

where $1 < L < N$ is the number of prioritized directions. Consider that $0 < T < 1$ is the normalized version of $T_{priority}$ used in the Algorithm 1, i.e. $T_{priority} = T\left(\sum_i \sum_j \sum_k \mathbf{H}(i,j,k)\right)$. Thus, the prioritized directions are chosen such that $\mathbf{P}_{s_k} > T$ for $k = 1, \ldots, L$. The parameter $0 < Q < 1$ characterizes an upper bound on the contribution of the non-prioritized beam directions to τ_1. This is achieved by ensuring that Q satisfies $\sum_{k=1}^{N-L} k(Q - \mathbf{P}_{s_{(k+L)}}) \geq 0$.

The following result describes conditions under which the average number of steps taken by Algorithm 1, τ_1, is less than the average number of steps taken in the benchmark case, τ_b.

Proposition 1. *If $Q < 1/N$ as well as $2L < N + 1$, and the priority threshold T satisfies that $T \geq Q$. Then, $\tau_1 < \tau_b$.*

Proof. In (3) a change of variable $j = k - L$ in the second summation produces

$$\tau_1 = \sum_{k=1}^{L} k\mathbf{P}_{s_k} + \sum_{j=1}^{N-L} j\mathbf{P}_{s_{(k+L)}} + L\sum_{j=L+1}^{N} \mathbf{P}_{s_j}. \tag{4}$$

Next, the last summation satisfies that $\sum_{j=L+1}^{N} \mathbf{P}_{s_j} = (1 - \sum_{k=1}^{L} \mathbf{P}_{s_k})$, thus after rearranging terms it follows that

$$\tau_1 = L - \sum_{k=1}^{L}(L-k)\mathbf{P}_{s_k} + \sum_{j=1}^{N-L} j\mathbf{P}_{s_{(j+L)}}. \tag{5}$$

The parameters T, Q and the term $(N+1)/2$ are introduced in the equation by adding zero as follows

$$\tau_1 = \frac{N+1}{2} - \frac{N+1}{2} + L - \sum_{k=1}^{L}(L-k)\left(\mathbf{P}_{s_k} - T + T\right) + \sum_{j=1}^{N-L} j\left(\mathbf{P}_{s_{(j+L)}} - Q + Q\right), \tag{6}$$

which can be written as

$$\tau_1 = -\frac{L(L-1)}{2}\left\{T - \left[Q - \left(\frac{1}{N} - Q\right)\left(\frac{N+1}{L} - 2\right)\frac{N}{L-1}\right]\right\} \frac{N+1}{2} - \sum_{k=1}^{L}(L-k)(\mathbf{P}_{s_k} - T) - \sum_{j=1}^{N-L} j(Q - \mathbf{P}_{s_{(j+L)}}). \tag{7}$$

A sufficient condition to guarantee that $\tau_1 < \tau_b$ is to ensure that the term inside the curly brackets in (7) is positive which is guaranteed with the conditions stated in Proposition 1. □

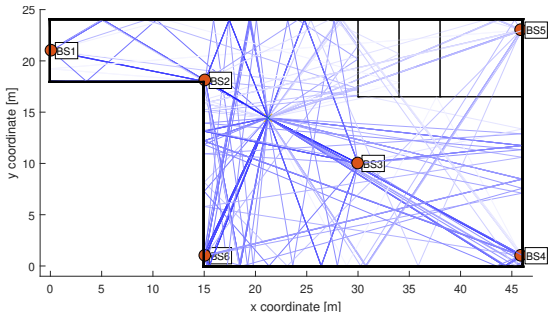

(a) Ray tracing for a UE

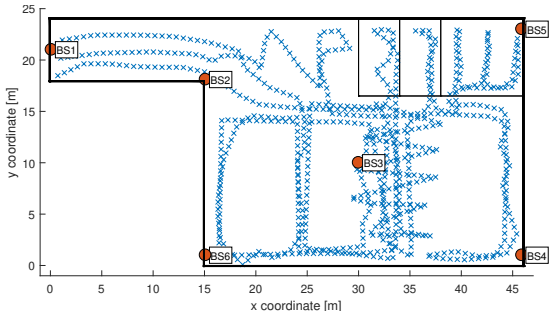

(b) UEs' locations

Fig. 1. Map of the indoor scenario

V. Ray tracing simulation

This section describes the collection and analysis of statistical data obtained from a mmW simulation.

A. Ray tracing simulator

Simulations are performed in a spatial modeling simulator based on the map-based model described in [10]. This map-based model provides accurate and realistic modeling of the spatial channel properties. The simulator uses ray tracing to model wave propagation and uses a simplified 3D geometry to describe propagation in the environment. The model considers diffraction, reflections, diffuse scattering and radio shadowing as described in [10]. The simulation map may contain buildings with vertical walls, convex objects, and other surfaces with arbitrary spatial orientation and propagation properties. Transmitters and receivers are defined by points in the map.

Given the 3D map, the simulator computes 2D rays on the xy-plane connecting transmitters and receivers. Single and double reflections are allowed. Next, the 2D rays are lifted from the xy-plane and the z-component is computed using basic geometric principles. Full 3D ray tracing is performed considering a few surfaces that were not considered during the 2D ray tracing step. The rays form paths connecting transmitters and receivers. Fig. 1a shows the paths going from several base stations to a UE. The next step is to compute the propagation properties for each path considering the effects of shadowing loss due to objects, free space path loss, reflections, diffraction and scattering. Finally, channel properties are computed by combining the paths using the radiation patterns of the transmitters and the receivers.

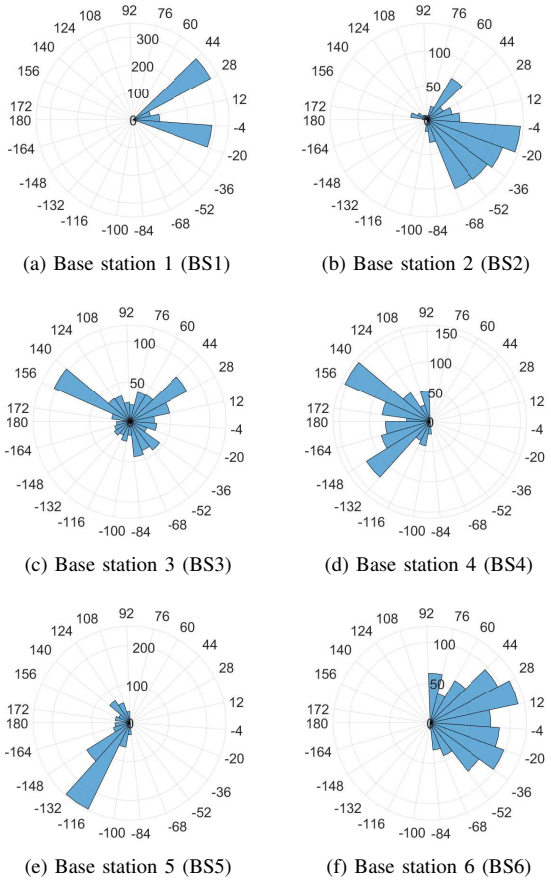

(a) Base station 1 (BS1)

(b) Base station 2 (BS2)

(c) Base station 3 (BS3)

(d) Base station 4 (BS4)

(e) Base station 5 (BS5)

(f) Base station 6 (BS6)

Fig. 2. Histograms for the azimuth component of the beam used to connect with the UEs.

B. Numerical simulation

Consider the indoor map depicted in Fig. 1 having 6 base stations. Statistics are collected over 791 simulations of UEs at fixed locations in a room with a flat floor and a roof height of $2.5m$. Fig. 1b shows the UEs' locations. The carrier frequency is 28 GHz. Beamforming is used by the UEs and by the base stations, with a 4×2 planar array used by the UEs and a 16×4 planar array for the base stations. This corresponds to beam widths of 33° in azimuth and 78° in elevation for the UEs and beam widths of 8° in azimuth and 33° in elevation for the base stations. The UEs' codebook is defined by beams pointing at 3 elevation angles $\{0°, 19°, 42°\}$ and 22 azimuth angles in the range $[0°, 343.6°]$ which give a UE codebook with 66 beam directions. For the base stations, the codebook is defined by 3 elevation angles $\{-42°, -19°, 0°\}$ and 45 azimuth angles in the range $[0°, 352°]$ which gives a codebook with 135 beam directions. For each UE the best beam combination that connects it with each base station is searched for. This provides the best direction for a base station to transmit a PRS for that UE (which is often given by line-of-sight between a UE and a base station). Next, this information is used to generate statistics of beam usage.

Single-site statistical data is analyzed for azimuth only. His-

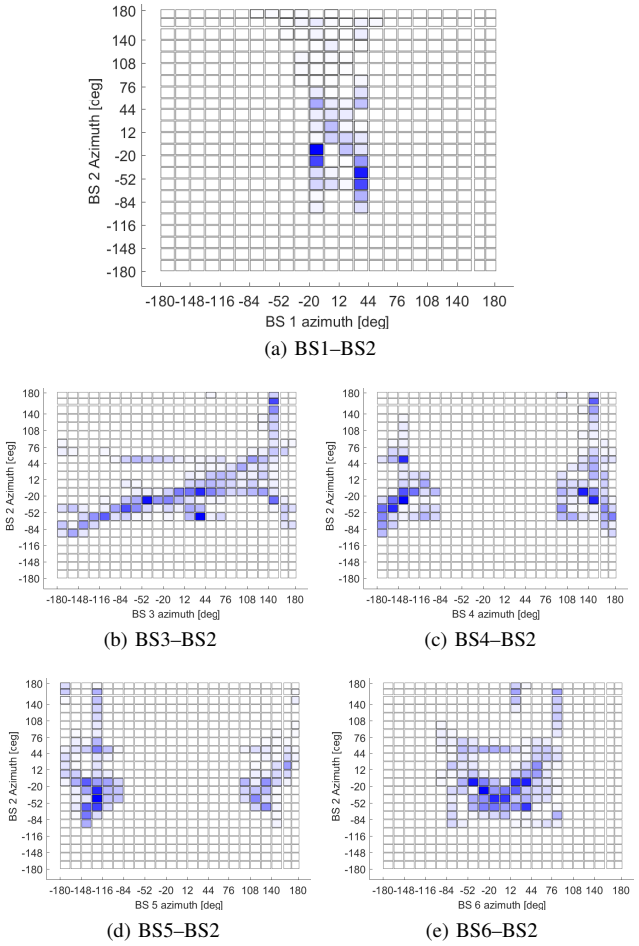

(a) BS1–BS2

(b) BS3–BS2

(c) BS4–BS2

(d) BS5–BS2

(e) BS6–BS2

Fig. 3. Multi-site histograms of the azimuth angle for the beams used for joint connection with UEs connected to base station 2 and other base stations.

tograms for each base station are generated using a partition in azimuth having 23 bins as shown in Fig. 2a-2f. For base station 1 (BS1), the histogram shown in Fig. 2a is dominated by two directions, one pointing at the corner on which base station 2 (BS2) is located and the direction on which that corner is reflected on the upper wall. Many UEs do not have line-of-sight with BS1 and thus the best link relies on diffraction at the inside corner at coordinates $x = 15$, $y = 18$. The histogram for BS2 shown in Fig. 2b is also influenced by the distribution of the UEs on the map with many directions having little usage. A similar pattern can be seen in Fig. 2c-2f for all other base stations.

Multi-site statistical data is also analyzed for azimuth only. Fig. 3a-3e show the histograms of the directions of BS2 when the UEs are also connected to other base stations. Pairs of beam directions that are used more often are denoted with dark blue rectangles, less used beam direction pairs have a light blue color, and beam direction pairs that were not used are denoted with white rectangles. The histogram for the pairs of beam directions used for joint connection with BS1 and BS2 is shown in Fig. 3a. Note that many UEs connected to BS1 with beam direction between $-20°$ and $-4°$ are connected to BS2 in the azimuth angles between $-36°$ and $-4°$. There is also a high correlation between BS1 azimuth angles in the range $[28°, 44°]$ and azimuth angles for BS2 in the range $[-84°, -20°]$. The histogram in Fig. 3a is sparse with only a few beam direction pairs dominating the histogram. Fig. 3b shows the histogram of the beam direction pairs used for joint connection with BS3 and BS2. This histogram shows that all possible BS3 azimuth angles values are observed, but many beam pairs for BS3 and BS2 are not observed. For example, the combination of azimuth angles for BS2 in the range $[108°, 180°]$ and azimuth angles for BS3 in the range $[-180°, 108°]$ were not used for joint connection, as evidenced by a wide white area in the left-upper part of Fig. 3b. Such an observation significantly reduces the space of possible beam direction pairs for BS3 and BS2. Similar observations can be made for the remaining histograms shown in Fig. 3c-3e.

VI. Conclusions

The paper proposes collection of statistical data about the beam directions used during successful positioning OTDOA attempts. This information helps to mitigate the beam search complexity that arises at mmW carrier frequencies when high directivity antenna arrays are used. A numerical study using ray tracing simulations show that a significant reduction in the search space of beam directions can be achieved with the proposed approach.

Acknowledgment

This research was supported under Australian Research Council's Linkage Projects funding scheme (project number LP150100757).

References

[1] T. S. Rappaport, S. Sun, R. Mayzus, H. Zhao, Y. Azar, K. Wang, G. N. Wong, J. K. Schulz, M. Samimi, and F. Gutierrez, "Millimeter wave mobile communications for 5G cellular: It will work!" *IEEE Access*, vol. 1, pp. 335–349, 2013.

[2] R. H. Middleton, T. Wigren, L. Boström, R. A. Delgado, K. Lau, R. S. Karlsson, L. Brus, and E. Corbett, "Feedback control applications in new radio: exploring delay control and alignment," *to appear in IEEE Vehicular Technology*, 2019.

[3] T. Samad, "Control systems and the internet of things," *IEEE Control Systems*, vol. 36, pp. 13–16, 2016.

[4] R. C. D. T. S. Rappaport, R. W. Heath Jr. and J. N. Murdock, *Millimeter wave wireless communications*. Westford, Massachusetts: Prentice Hall, 2014.

[5] A. Kangas, I. Siomina, and T. Wigren, "Positioning in LTE," in *Handbook of Position Location*. John Wiley & Sons, Inc., Sep. 2011, pp. 1081–1127.

[6] T. Wigren, "Wireless hybrid positioning based on surface modeling with polygon support," in *2018 IEEE 87th Vehicular Technology Conference (VTC Spring)*. Porto, Portugal: IEEE, Jun. 2018.

[7] T. Wigren, I. Siomina, and M. Anderson, "Estimation of prior positioning method performance in LTE," in *2011 IEEE 22nd International Symposium on Personal, Indoor and Mobile Radio Communications*. IEEE, Sep. 2011.

[8] Y. Liu, X. Shi, S. He, and Z. Shi, "Prospective positioning architecture and technologies in 5G networks," *IEEE Network*, vol. 31, no. 6, pp. 115–121, Nov. 2017.

[9] E. D. Kaplan, *Understanding GPS - principles and applications*. Artech House, 1996.

[10] V. Nurmela *et al.*, "Deliverable D1.4: METIS channel models," Mobile Wireless Commun. Enablers Twenty-Twenty Inf. Soc. (METIS), Jun. 2015.